

Generation of nonlinear currents and low-frequency radiation upon interaction of a laser pulse with a metal

S.G. Bezhanov, S.A. Uryupin

Abstract. Nonlinear currents slowly varying in time are found in the skin layer of a metal irradiated by short laser pulses. The low-frequency field generated by the nonlinear currents in metal and vacuum is studied. The spectral composition, energy and shape of the low-frequency radiation pulse are described.

Keywords: femtosecond pulse, nonlinear current, skin layer, terahertz radiation.

1. Introduction

The study of the generation of nonlinear currents and emerging low-frequency fields began in the early years of nonlinear optics development. Due to the progress in obtaining femtosecond laser pulses, this part of nonlinear optics has been further developed due to the ability to produce sufficiently strong fields in the skin layer in a time shorter than the time of significant heating of the electrons and the lattice, resulting in the destruction of the surface of the metal. Recently, interest in this area of research has increased due to new opportunities in mastering the terahertz frequency range. Generation of terahertz radiation on the surface of silver and gold was observed in [1, 2], and on the surface of copper – in [3]. The authors of [4] studied terahertz radiation upon irradiation of semiconductors in a magnetic field. It was shown in [5] that when a femtosecond laser pulse interacts with a nanostructured metal surface, the efficiency of terahertz radiation generation increases significantly. The emergence of new experimental works points to the need for a theory capable of adequate description of the observed patterns of terahertz radiation generation. The appropriate step in this direction has been made in this paper in relation to the description of the properties of the interaction of a femtosecond s-polarised pulse with a gold target (found in [1, 2]).

In Section 2 we investigate the field generated in a metal by a short s-polarised pulse. Nonlinear currents in the skin layer and the low-frequency field in the metal are considered in Section 3. The field of low-frequency radiation in a vacuum is described in Section 4. We also present the expressions for the Fourier transforms of the magnetic field in vacuum, the explicit form of which depends on the relations between the

frequency of collisions between electrons and the frequencies of the fundamental and generated fields. The spectral composition, energy and shape of the low-frequency pulse are considered in Section 5. We show that when the metal is irradiated by a femtosecond s-polarised pulse, broadband terahertz radiation is generated. The most efficient generation occurs at a frequency on the order of the inverse duration of the fundamental femtosecond pulse. The low-frequency pulse duration is comparable to the duration of the fundamental pulse, and the total energy of low-frequency radiation is proportional to the square of the fundamental radiation intensity. We present an explanation of the frequency and temporal characteristics of the low-frequency pulse, obtained in [1, 2]. We have found that in this case it is necessary to consider the collision of electrons, leading to the generation of a nonlinear current along the metal surface.

2. High-frequency field

Consider the interaction of an electromagnetic s-polarised pulse with a metal occupying the half-space $z > 0$. Electric and magnetic fields of the pulse incident on the metal surface have the form

$$\begin{aligned} \mathbf{E}_{\text{inc}}(\mathbf{r}, t) &= \frac{1}{2} \mathbf{E}_{\text{inc}}(t - \mathbf{kr}/\omega) \exp(-i\omega t + i\mathbf{kr}) + \text{c. c.}, \\ \mathbf{B}_{\text{inc}}(\mathbf{r}, t) &= \frac{1}{2} \mathbf{B}_{\text{inc}}(t - \mathbf{kr}/\omega) \exp(-i\omega t + i\mathbf{kr}) + \text{c. c.}, \end{aligned} \quad (1)$$

where $\mathbf{E}_{\text{inc}}(t - \mathbf{kr}/\omega) = E_{\text{inc}}(t - \mathbf{kr}/\omega)(0, 1, 0)$; $\mathbf{B}_{\text{inc}}(t - \mathbf{kr}/\omega) = E_{\text{inc}}(t - \mathbf{kr}/\omega)(-\cos\theta, 0, \sin\theta)$; ω is the carrier frequency; θ is the angle between the direction of the pulse propagation and the vector of the external normal to the surface of the metal; $\mathbf{k} = (\omega/c)(\sin\theta, 0, \cos\theta)$ is the wave vector; and c is the velocity of light. We also assume that the function $E_{\text{inc}}(t - \mathbf{kr}/\omega)$ weakly changes over the time $\sim 1/\omega$.

In describing the response of the metal to the action of the field of form (1) under conditions when the frequency ω or the electron collision frequency is greater than the ratio of the Fermi velocity v_F to the skin-layer depth, we will use the equation for the velocity $\mathbf{u} = \mathbf{u}(\mathbf{r}, t)$ of the directed motion of the electrons

$$\frac{\partial \mathbf{u}}{\partial t} + (\mathbf{u} \nabla) \mathbf{u} = \frac{\mathbf{f}}{m} + \frac{e}{m} \left(\mathbf{E} + \frac{1}{c} [\mathbf{u} \mathbf{B}] \right) - \frac{1}{mn} \nabla p, \quad (2)$$

where $\mathbf{f} = \mathbf{f}(\mathbf{r}, t)$ is the friction force; e and m are the charge and effective mass of the electron; $\mathbf{E} = \mathbf{E}(\mathbf{r}, t)$ and $\mathbf{B} = \mathbf{B}(\mathbf{r}, t)$ are the electric and magnetic fields in the metal; and p and n

S.G. Bezhanov, S.A. Uryupin P.N. Lebedev Physics Institute, Russian Academy of Sciences, Leninsky prosp. 53, 119991 Moscow, Russia; National Research Nuclear University 'MEPhI', Kashirskoe sh. 31, 115409 Moscow, Russia; e-mail: uryupin@sci.lebedev.ru

Received 2 July 2013; revision received 1 August 2013
Kvantovaya Elektronika 43 (11) 1048–1054 (2013)
Translated by I.A. Ulitkin

are the pressure and concentration of the electrons. The field in the metal is described by Maxwell's equations

$$\text{rot}\mathbf{E} = -\frac{1}{c}\frac{\partial\mathbf{B}}{\partial t}, \quad \text{rot}\mathbf{B} = \frac{1}{c}\frac{\partial\mathbf{D}}{\partial t} + \frac{4\pi}{c}\mathbf{j}, \quad (3)$$

where $\mathbf{D} = \mathbf{D}(\mathbf{r}, t)$ is the electric displacement field. The current density $\mathbf{j} = \mathbf{j}(\mathbf{r}, t) = en\mathbf{u}(\mathbf{r}, t)$, the velocity \mathbf{u} , the friction force \mathbf{f} and the fields in the metal we present in the form

$$\mathbf{F} = \mathbf{F}(\mathbf{r}, t) = \mathbf{F}_0(\mathbf{r}, t) + \frac{1}{2}[\mathbf{F}_1(\mathbf{r}, t)\exp(-i\omega t) + \text{c. c.}], \quad (4)$$

where $\mathbf{F} = \mathbf{E}, \mathbf{B}, \mathbf{D}, \mathbf{f}, \mathbf{u}, \mathbf{j}$; and the function $F_n = F_n(\mathbf{r}, t)$ weakly changes over the time $\sim 1/\omega$,

$$\omega \gg \left| \frac{\partial}{\partial t} \ln F_n \right|. \quad (5)$$

In formula (4) we omitted the harmonics $\exp(-in\omega t)$ with numbers $n \geq 2$, which is justified in a sufficiently weak field.

Taking into account the field weakness and inequality (5), from (2) for $\mathbf{j}_1(\mathbf{r}, t)$ we find the approximate expression

$$\mathbf{j}_1(\mathbf{r}, t) = \frac{i\omega_p^2}{4\pi(\omega + iv)}\mathbf{E}_1(\mathbf{r}, t), \quad (6)$$

where $\omega_p = \sqrt{4\pi ne^2/m}$ is the plasma frequency and v is the collision frequency of the electrons interacting with the high-frequency electromagnetic field. In deriving relation (6) we used a simple expression for the force of friction: $\mathbf{f}_1(\mathbf{r}, t) = -mv\mathbf{u}_1(\mathbf{r}, t)$.

In expression (3), the difference of $\mathbf{D}(\mathbf{r}, t)$ from $\mathbf{E}(\mathbf{r}, t)$ is due to the influence of the lattice and bound electrons. This difference is described by the ω -frequency dependent dielectric constant $\varepsilon_0(\omega)$. In particular, at frequencies close to ω frequencies, we have

$$\begin{aligned} \mathbf{D}_1(\mathbf{r}, t)\exp(-i\omega t) &= \int_{-\infty}^t \varepsilon_0(t-t')\mathbf{E}_1(\mathbf{r}, t')\exp(-i\omega t')dt' \\ &\simeq \varepsilon_0(\omega)\mathbf{E}_1(\mathbf{r}, t)\exp(-i\omega t), \end{aligned} \quad (7)$$

where

$$\varepsilon_0(\omega) = \int_0^\infty \varepsilon_0(t)\exp(i\omega t)dt$$

and the weak change in $\mathbf{E}_1(\mathbf{r}, t)$ over the time $\sim 1/\omega$ is neglected.

Taking into account expressions (4)–(7) under the condition of the action of s-polarised radiation for the function $\mathbf{E}_1(\mathbf{r}, t)$ determining the field in the metal, we derive from (3) the relation

$$\Delta\mathbf{E}_1(\mathbf{r}, t) + \frac{\omega^2}{c^2}\varepsilon(\omega)\mathbf{E}_1(\mathbf{r}, t) = 0, \quad (8)$$

where $\varepsilon(\omega) = \varepsilon_0(\omega) - \omega_p^2/[\omega(\omega + iv)]$. We will seek the approximate solution of equation (8) in the form $\mathbf{E}_1(\mathbf{r}, t) = (0, E_1(\mathbf{r}, t), 0)$, where

$$E_1(\mathbf{r}, t) \simeq E_1(z, x, t)\exp(ikx \sin \theta). \quad (9)$$

Then, by neglecting the weak changes in $E_1(z, x, t)$ along the surface of the metal, from (8) we obtain the approximate equation

$$\frac{\partial^2}{\partial z^2}E_1(z, x, t) - \kappa^2 E_1(z, x, t) = 0, \quad (10)$$

where we use the notation

$$\kappa^2 = \frac{\omega^2}{c^2}[\sin^2 \theta - \varepsilon(\omega)] = \text{Re}\kappa^2 - i\text{Im}\kappa^2. \quad (11)$$

By assuming $\text{Re}\kappa^2 > 0$ and $\text{Im}\kappa^2 > 0$, the solution of equation (10) decreasing into the metal bulk can be written as

$$E_1(z, x, t) = E_1(0, x, t)\exp(-\kappa z), \quad \kappa = \kappa_1 - i\kappa_2, \quad (12)$$

$$\kappa_p = \frac{1}{\sqrt{2}}[\sqrt{(\text{Re}\kappa^2)^2 + (\text{Im}\kappa^2)^2} - (-1)^p \text{Re}\kappa^2]^{1/2}, \quad p = 1, 2.$$

In turn, from (3), (4), (9) and (12) for the function $\mathbf{B}_1(\mathbf{r}, t)$ determining the magnetic field in the metal we have the relation

$$\mathbf{B}_1(\mathbf{r}, t) = E_1(0, x, t)\exp(-\kappa z + ikx \sin \theta)\left(-i\frac{\kappa}{k}, 0, \sin \theta\right). \quad (13)$$

Electromagnetic radiation is partially reflected from the metal. Taking into account inequality (5), in the approximation linear in E_{inc} , the fields of the reflected s-polarised pulse have the form

$$\begin{aligned} \mathbf{E}_{\text{ref}}(\mathbf{r}, t) &= \frac{1}{2}\mathbf{E}_{\text{ref}}(t - \mathbf{k}'\mathbf{r}/\omega)\exp(-i\omega t + i\mathbf{k}'\mathbf{r}) + \text{c. c.}, \\ \mathbf{B}_{\text{ref}}(\mathbf{r}, t) &= \frac{1}{2}\mathbf{B}_{\text{ref}}(t - \mathbf{k}'\mathbf{r}/\omega)\exp(-i\omega t + i\mathbf{k}'\mathbf{r}) + \text{c. c.}, \end{aligned} \quad (14)$$

where $\mathbf{E}_{\text{ref}}(t - \mathbf{k}'\mathbf{r}/\omega) = R\mathbf{E}_{\text{inc}}(t - \mathbf{k}'\mathbf{r}/\omega)$; R is the complex reflection coefficient; $\mathbf{k}' = k(\sin \theta, 0, -\cos \theta)$; and $\mathbf{B}_{\text{ref}}(t - \mathbf{k}'\mathbf{r}/\omega) = R\mathbf{E}_{\text{inc}}(t - \mathbf{k}'\mathbf{r}/\omega)(\cos \theta, 0, \sin \theta)$.

Using the condition of continuity of the tangential components of the electric and magnetic fields, from relations (1), (4), (9), (12), (13) and (14) we find the complex coefficients of penetration (F_s) and reflection (R) of s-polarised radiation:

$$F_s \simeq \frac{2k \cos \theta}{k \cos \theta + i\kappa}, \quad R \simeq \frac{k \cos \theta - i\kappa}{k \cos \theta + i\kappa}, \quad (15)$$

and the function $E_1(0, x, t)$:

$$E_1(0, x, t) = F_s E_{\text{inc}}\left(t - \frac{x \sin \theta}{c}\right). \quad (16)$$

Formulas (4), (9), (11)–(13) and (16) define a high-frequency field in the metal.

3. Nonlinear current and low-frequency field in the metal

Consider an electromagnetic field and current density at frequencies Ω , much smaller than ω . At low frequencies, the fric-

tion force f_0 depends on the electron collision frequency ν_s , which differs from ν : $f_0 = -mv_s u_0$. Keeping in mind this difference, in the case of the action of the s-polarised pulse we derive from (2) and (4)

$$\begin{aligned} \frac{\partial j_0(\mathbf{r}, t)}{\partial t} + \nu_s j_0(\mathbf{r}, t) &= \frac{\omega_p^2}{4\pi} E_0(\mathbf{r}, t) \\ &+ \frac{e}{4mc} \{ [j_1(\mathbf{r}, t) \mathbf{B}_1^*(\mathbf{r}, t)] + [j_1^*(\mathbf{r}, t) \mathbf{B}_1(\mathbf{r}, t)] \}. \end{aligned} \quad (17)$$

In (17) the contribution of the pressure changes is omitted. This approximation is justified if, for the frequencies Ω considered below, conditions of the high-frequency or normal skin effect are realised. Below, using expressions for j_1 (6), \mathbf{E}_1 (9), (12), (16) and \mathbf{B}_1 (13), after the Fourier transform in time ($t \rightarrow \Omega$) and coordinate x ($x \rightarrow q$), we have from (17)

$$\begin{aligned} -i(\Omega + i\nu_s) j_0(q, z, \Omega) &= \frac{\omega_p^2}{4\pi} E_0(q, z, \Omega) \\ &+ \nu J(q, \Omega) \exp(-2\kappa_1 z). \end{aligned} \quad (18)$$

Here we use the notations $\mathbf{J}(q, \Omega) = (J_x(q, \Omega), 0, J_z(q, \Omega))$,

$$J_x(q, \Omega) = \frac{e\omega_p^2 \sin\theta}{mc^2 \omega^2 + \nu^2} |F_s|^2 I(\Omega) 2\pi \delta\left(q - \frac{\Omega \sin\theta}{c}\right), \quad (19)$$

$$J_z(q, \Omega) = \frac{e\omega_p^2}{mc\nu\omega} \frac{\omega\kappa_1 + \nu\kappa_2}{\omega^2 + \nu^2} |F_s|^2 I(\Omega) 2\pi \delta\left(q - \frac{\Omega \sin\theta}{c}\right), \quad (20)$$

where $\delta(x)$ is the delta function, and $I(\Omega)$ is the Fourier transform of the energy flux density:

$$I(\Omega) = \frac{c}{8\pi} \int_{-\infty}^{\infty} d\tau E_{\text{inc}}^2(\tau) \exp(i\Omega\tau). \quad (21)$$

According to (18), if we omit the term with $\mathbf{E}_0(q, z, \Omega)$, then the function $\mathbf{J}(q, \Omega)$ defines the Fourier transform of the drag current density [6]. Taking into account relations (4), from Maxwell's equations (3) for the Fourier transform of the slowly varying magnetic field $\mathbf{B}_0(q, z, \Omega) = (0, B_0(q, z, \Omega), 0)$ we obtain the equation

$$\frac{d^2}{dz^2} B_0(q, z, \Omega) - \kappa_s^2 B_0(q, z, \Omega) = Q(q, \Omega) \exp(-2\kappa_1 z), \quad (22)$$

where

$$Q(q, \Omega) = \frac{4i\pi\nu}{c(\Omega + i\nu_s)} [2\kappa_1 J_x(q, \Omega) + iqJ_z(q, \Omega)], \quad (23)$$

$$\kappa_s^2 = q^2 - \frac{\Omega^2}{c^2} \varepsilon(\Omega) \equiv \text{Re}\kappa_s^2 - i\text{Im}\kappa_s^2, \quad (24)$$

$$\varepsilon(\Omega) = \varepsilon_0(\Omega) - \frac{\omega_p^2}{\Omega(\Omega + i\nu_s)} = \varepsilon'(\Omega) + i\varepsilon''(\Omega). \quad (25)$$

Typically, $\text{Re}\kappa_s^2 > 0$. The solution to equation (22), decreasing with distance from the surface of the metal, has the form

$$\begin{aligned} B_0(q, z, \Omega) &= B(q, 0, \Omega) \exp(-\kappa_s z) \\ &+ \frac{Q(q, \Omega)}{4\kappa_1^2 - \kappa_s^2} [\exp(-2\kappa_1 z) - \exp(-\kappa_s z)], \end{aligned} \quad (26)$$

$$\kappa_s = \kappa_{s1} - i\kappa_{s2} \text{sign}(\text{Im}\kappa_s^2),$$

$$\kappa_{sp} = \frac{1}{\sqrt{2}} [\sqrt{(\text{Re}\kappa_s^2)^2 + (\text{Im}\kappa_s^2)^2} - (-1)^p \text{Re}\kappa_s^2]^{1/2}, p = 1, 2, \quad (27)$$

where $B(q, 0, \Omega)$ is the value of the function $B_0(q, z, \Omega)$ at $z = 0$. By using relation (26) and the second expression from equations (3), we find the Fourier transforms of the electric field components:

$$\begin{aligned} E_{0x}(q, z, \Omega) &= \frac{ic}{\varepsilon(\Omega)\Omega} \left\{ B(q, 0, \Omega) \kappa_s \exp(-\kappa_s z) \right. \\ &+ \frac{Q(q, \Omega)}{4\kappa_1^2 - \kappa_s^2} [2\kappa_1 \exp(-2\kappa_1 z) - \kappa_s \exp(-\kappa_s z)] \\ &\left. - \frac{4\pi}{c} \frac{i\nu}{\Omega + i\nu_s} J_x(q, \Omega) \exp(-2\kappa_1 z) \right\}, \end{aligned} \quad (28)$$

$$\begin{aligned} E_{0z}(q, z, \Omega) &= -\frac{c}{\varepsilon(\Omega)\Omega} \left\{ B(q, 0, \Omega) q \exp(-\kappa_s z) \right. \\ &+ \frac{Q(q, \Omega)}{4\kappa_1^2 - \kappa_s^2} q [\exp(-2\kappa_1 z) - \exp(-\kappa_s z)] \\ &\left. - \frac{4\pi}{c} \frac{\nu}{\Omega + i\nu_s} J_z(q, \Omega) \exp(-2\kappa_1 z) \right\}. \end{aligned} \quad (29)$$

The functions $B_0(q, z, \Omega)$ (26), $E_{0x}(q, z, \Omega)$ (28) and $E_{0z}(q, z, \Omega)$ (29) allow us to describe the field in the metal at frequencies much lower than ω .

4. Low-frequency radiation field

In a vacuum, for the Fourier transform of the magnetic field $\mathbf{B}_r(q, z, \Omega) = (0, B_r(q, z, \Omega), 0)$ from system (3) we obtain the equation

$$\frac{d^2}{dz^2} B_r(q, z, \Omega) + \left(\frac{\Omega^2}{c^2} - q^2 \right) B_r(q, z, \Omega) = 0. \quad (30)$$

The solution to this equation, corresponding to the wave escaping from the metal surface, has the form

$$B_r(q, z, \Omega) = B_r(q, 0, \Omega) \exp\left(-iz\sqrt{\frac{\Omega^2}{c^2} - q^2}\right). \quad (31)$$

In this case, for the components $E_{rx}(q, z, \Omega)$ and $E_{rz}(q, z, \Omega)$ we obtain the relations

$$E_{rx}(q, z, \Omega) = -\sqrt{1 - \frac{q^2 c^2}{\Omega^2}} B_r(q, z, \Omega), \quad (32)$$

$$E_{rz}(q, z, \Omega) = -\frac{qc}{\Omega} B_r(q, z, \Omega). \quad (33)$$

The comparison of formulas (29) and (33) shows that $\varepsilon(\Omega)E_{0z}(q, 0, \Omega) \neq E_{rz}(q, 0, \Omega)$ at $z = 0$. The absence of continu-

ity of the normal component of the Fourier transform of the electric induction is the result of an approximate description of the nonlinear current. However, under conditions $\max(\Omega, v_s) \gg |\kappa_s|v_F$, when considering the generation of low-frequency radiation, a precise description of the z -component of the electric field is not necessary. It is enough to satisfy the conditions of continuity of the tangential components of the electric and magnetic fields that lead to the relations

$$B_r(q, 0, \Omega) = B(q, 0, \Omega), \quad (34)$$

$$i\varepsilon(\Omega)\sqrt{\frac{\Omega^2}{c^2} - q^2} B_r(q, 0, \Omega) = \kappa_s B(q, 0, \Omega) + \frac{Q(q, \Omega)}{2\kappa_1 + \kappa_s} - \frac{4\pi}{c} \frac{iv}{\Omega + iv_s} J_x(q, \Omega). \quad (35)$$

By using (23), we find from equations (34) and (35) the Fourier transform of the magnetic field on the surface of the metal

$$B_r(q, 0, \Omega) = \frac{4\pi}{c} \frac{v}{(\Omega + iv_s)(2\kappa_1 + \kappa_s)} \frac{iqJ_z(q, \Omega) - \kappa_s J_x(q, \Omega)}{[\varepsilon(\Omega)\sqrt{\Omega^2/c^2 - q^2} + i\kappa_s]}. \quad (36)$$

Taking into account the relations (19), (20) and (31), after the inverse Fourier transform in q we derive from (36)

$$B_r(\mathbf{r}, \Omega) = \frac{-16\pi\omega_p^2 k^2 \sin\theta \cos^2\theta [\kappa_s v - i\Omega(\kappa_1 + \kappa_2 v/\omega)]}{mc^2(\Omega + iv_s)(2\kappa_1 + \kappa_s)(\omega^2 + v^2) [\varepsilon(\Omega)\Omega \cos\theta + i\kappa_s] |k \cos\theta + i\kappa|^2} \times I(\Omega) \exp\left[i\frac{\Omega}{c}(x \sin\theta - z \cos\theta)\right]. \quad (37)$$

According to (37), the radiation of the metal at low frequencies occurs at an angle θ , i.e., in the direction of reflection of the fundamental high-frequency signal. Formulas (36) and (37) take into account the collisions of the electrons. This refinement has led to the emergence of a nonlinear, emitting low-frequency current along the surface of the metal. Note that Kadlec et al. [2] take into account only the nonlinear susceptibility, corresponding to the current along the normal to the metal surface. We will show below that under conditions of interest, including those realised in [2], both currents are comparable in magnitude and important for the description of the low-frequency response of the metal.

Expression (37) can be considerably simplified. Often, the carrier frequency of the fundamental pulse satisfies the inequalities $\omega_p \gg \omega \gg v$ and $\omega_p^2 \gg \omega^2 |\varepsilon_0(\omega)|$. Moreover, $\omega \gg \omega_p v_F/c$. Under such conditions, $\kappa \simeq \kappa_1 \simeq \omega_p/c$. At a frequency Ω , it is relatively easy to implement the inequality $\omega_p^2 \gg |\varepsilon_0(\Omega)(\Omega + iv_s)\Omega|$. Thus, $\kappa_s \simeq (\omega_p/c)\sqrt{\Omega/(\Omega + iv_s)}$. Taking into account the presented inequalities at $\Omega \gg v_s$, we obtain from (37)

$$B_r(\mathbf{r}, \Omega) \simeq \frac{16\pi}{3} \frac{e}{mc^2 \omega_p^2} \frac{v - i\Omega}{(\cos\theta - i\Omega/\omega_p)} \sin\theta \cos^2\theta \times I(\Omega) \exp\left[i\frac{\Omega}{c}(x \sin\theta - z \cos\theta)\right], \quad \omega \gg v. \quad (38)$$

At lower frequencies, when $v_s \gg \Omega$, expression (37) takes the form

$$B_r(\mathbf{r}, \Omega) = 8\pi \frac{e}{mc^2 \omega_p^2} \frac{[v(1-i)\sqrt{\Omega/(2v_s)} - i\Omega]}{[\cos\theta + (1-i)\sqrt{\Omega v_s/(2\omega_p^2)}]} \sin\theta \cos^2\theta \times I(\Omega) \exp\left[i\frac{\Omega}{c}(x \sin\theta - z \cos\theta)\right], \quad \omega \gg v. \quad (39)$$

Under the conditions discussed, $\omega_p \gg \Omega$, $\sqrt{\Omega v_s}$ and the function $B_r(\mathbf{r}, \Omega)$ [(38) and (39)] has a maximum at $\theta \simeq \pi/4$. If $\Omega \gg v_s$, v , then according to (38) the generation of the low-frequency field is mainly determined by the nonlinear current proportional to J_z . On the contrary, if $\Omega \ll v_s$ and $v \gg \sqrt{\Omega v_s}$, then according to (39) the main contribution to the generated field is caused by the current driven along the x axis. Thus, in a wide range of angles θ , not close to $\pi/2$, expression (39) contains a large factor proportional to $v/\sqrt{\Omega v_s}$, which suggests a more efficient generation of low-frequency radiation in the limit of relatively high frequencies of collisions between the electrons. The same conclusion follows from formula (38) if $v > \Omega$.

Relations (38) and (39) correspond to the commonly encountered conditions in which $\omega \gg v$. If the collision frequency is so large that inequality $v \gg \omega$ is realised, then, generally speaking, there may be two limiting cases. Then, if $v \gg \omega \gg \Omega \gg v_s$, from (37) we have

$$B_r(\mathbf{r}, \Omega) \simeq 16\pi \frac{e\omega}{mc^2 \omega_p^2} \frac{\sin\theta \cos^2\theta}{\cos\theta - i\Omega/\omega_p} \times I(\Omega) \exp\left[i\frac{\Omega}{c}(x \sin\theta - z \cos\theta)\right]. \quad (40)$$

The inequality $v_s \ll v$, for example, can be realised due to a significant increase in the frequency of electron–electron collisions in a high-frequency field [7].

In the other limiting case, $v \gg \omega$ and $v_s \gg \Omega$. In this case, from (37) we obtain

$$B_r(\mathbf{r}, \Omega) \simeq 8\pi(1-i) \frac{e\sqrt{\Omega\omega}}{mc^2 \omega_p^2} \sqrt{\frac{v}{v_s}} \frac{\sin\theta \cos^2\theta}{\cos\theta + (1-i)\sqrt{\Omega v_s/(2\omega_p^2)}} \times I(\Omega) \exp\left[i\frac{\Omega}{c}(x \sin\theta - z \cos\theta)\right]. \quad (41)$$

In writing (41) we take into account the inequality $\Omega v \ll \omega v_s$. At θ , not close to $\pi/2$, in contrast to (40), expression (41) contains the parameter $\sqrt{\Omega v/(\omega v_s)}$, which is usually small. It is clear that with such θ , the function $B_r(\mathbf{r}, \Omega)$ is proportional to $\sqrt{v/v_s}$. Therefore, when v and v_s are close, expression (41) depends weakly on the electron collision frequency.

5. Spectral composition, energy and low-frequency radiation field

The energy of low-frequency radiation emitted from the unit area of the metal surface, is given by the time integral of the modulus of the Poynting vector:

$$W = \int_{-\infty}^{\infty} dt \frac{c}{4\pi} |\mathbf{E}_r(\mathbf{r}, t) \mathbf{B}_r(\mathbf{r}, t)| \equiv \int_0^{\infty} W(\Omega) d\Omega, \quad (42)$$

where

$$W(\Omega) = \frac{c}{4\pi^2} |\mathbf{B}_t(\mathbf{r}, \Omega)|^2 \quad (43)$$

is the spectral energy density. Using relations (12), (25), (27), (37) and definition (43), for $W(\Omega)$ we derive the expression

$$W(\Omega) = \frac{64e^2k^4\omega_p^4I^2(\Omega)}{m^2c^3(\Omega^2 + v_s^2)(\omega^2 + v^2)^2} \times \frac{\{\kappa_{s1}^2v^2 + [\kappa_{s2}v + \Omega(\kappa_1 + \kappa_2v/\omega)]^2\}}{(2\kappa_1 + \kappa_{s1})^2 + \kappa_{s2}^2} \{[\varepsilon'(\Omega)\Omega\cos\theta + c\kappa_{s2}]^2 + [\varepsilon''(\Omega)\Omega\cos\theta + c\kappa_{s1}]^2\}^{-1} \frac{\sin^2\theta\cos^4\theta}{[\kappa_1^2 + (\kappa_2 + k\cos\theta)^2]^2}. \quad (44)$$

In the above limiting cases and for the angles θ , not close to $\pi/2$, expression (44) can be considerably simplified. Using expressions (38)–(41), from (43) we obtain

$$W(\Omega) = \frac{64}{9c} \left(\frac{e}{m\omega_p^2} \right)^2 (v^2 + \Omega^2) I^2(\Omega) \sin^2\theta \cos^2\theta, \quad \Omega \gg v_s, \omega \gg v, \quad (45)$$

$$W(\Omega) = \frac{16}{c} \left(\frac{e}{m\omega_p^2} \right)^2 \left[\left(\Omega + v\sqrt{\frac{\Omega}{2v_s}} \right)^2 + \frac{v^2\Omega}{2v_s} \right] I^2(\Omega) \sin^2\theta \cos^2\theta, \quad \Omega \ll v_s, \omega \gg v, \quad (46)$$

$$W(\Omega) = \frac{64}{c} \left(\frac{e\omega}{m\omega_p^2} \right)^2 I^2(\Omega) \sin^2\theta \cos^2\theta, \quad v \gg \omega \gg \Omega \gg v_s, \quad (47)$$

$$W(\Omega) = \frac{32}{c} \left(\frac{e}{m\omega_p^2} \right)^2 \Omega \omega \frac{v}{v_s} I^2(\Omega) \sin^2\theta \cos^2\theta, \quad v \gg \omega, v_s \gg \Omega. \quad (48)$$

Relations (44)–(48) allow us to analyse the spectral composition of the low-frequency radiation, if the shape of the high-frequency pulse acting on the metal is specified. For example, it is possible in the case of a Gaussian pulse, $E_{\text{inc}}^2(\tau) = E_L^2 \exp(-\tau^2/\tau_p^2)$, where the time τ_p defines the pulse duration $t_p = 2\tau_p \sqrt{\ln 2}$. The Fourier transform of the energy flux density (21), responsible for such a pulse, has the form

$$I(\Omega) = \sqrt{\pi} \tau_p I_L \exp(-\Omega^2 \tau_p^2/4), \quad (49)$$

where $I_L = cE_L^2/(8\pi)$ is the maximum energy flux density.

Let us present numerical estimates for a gold target. We assume that the femtosecond pulse is produced by radiation of a Ti:sapphire laser with a carrier frequency $\omega \simeq 2.3 \times 10^{15} \text{ s}^{-1}$. The maximum energy flux density, I_L , will be chosen equal to $10^{12} \text{ W cm}^{-2}$ such that the pulse duration $t_p \sim 20 \text{ fs}$ provides no substantial heating of the electrons, and hence constant frequency of collisions. The time $\tau_p = t_p/(2\sqrt{\ln 2})$ satisfies the relation $\omega\tau_p \gg 1$, which allows us to consider the change in the field amplitude over the time $\sim 1/\omega$ to be slow. The angle of incidence on the metal is $\theta = \pi/4$. The plasma frequency for gold is $\omega_p = 1.37 \times 10^{16} \text{ s}^{-1}$. At a temperature $T = 300 \text{ K}$ use is made of the electron collision frequency $v = 1.2 \times 10^{14} \text{ s}^{-1}$ [8] and $v_s = 3.7 \times 10^{13} \text{ s}^{-1}$ [9]. According to the data

of Ref. [8] the value of $\varepsilon_0(\omega)$ corresponding to the frequency $\omega \simeq 2.3 \times 10^{15} \text{ s}^{-1}$ is ~ 8 .

Figure 1 shows the dependences of the spectral energy density $W(\Omega)$ (44) for various pulse durations t_p . The function $W(\Omega)$ is normalised to its maximum value W_{max} , achieved at $t_p = 15 \text{ fs}$. The generation efficiency at low frequencies is small. With increasing Ω , the function $W(\Omega)$ increases, reaches a maximum at $\Omega \sim 1/\tau_p$ and then decreases monotonically. Thus, the shorter the pulse, the greater the generation efficiency. Figure 2 shows similar dependences, which are plotted in the case of irradiation of an aluminium target at $v = 9.3 \times 10^{13} \text{ s}^{-1}$ [10], $v_s = 1.62 \times 10^{14} \text{ s}^{-1}$ [9], $\omega_p = 1.9 \times 10^{16} \text{ s}^{-1}$ [10] and $\varepsilon_0(\omega) \simeq 4 + 42i$ [11]. Despite the similarity of the curves in Figs 1 and 2 we can see that for aluminium the function $W(\Omega)/W_{\text{max}}$, with increasing pulse duration, decreases noticeably stronger.

The spectrum of terahertz radiation, such as the one presented in Fig. 1, is given in [2], where the authors studied experimentally the generation of low-frequency radiation on the surface of a gold target exposed to the radiation of a ~ 50 -fs, 810-nm Ti:sapphire. However, according to Fig. 1 [2], the

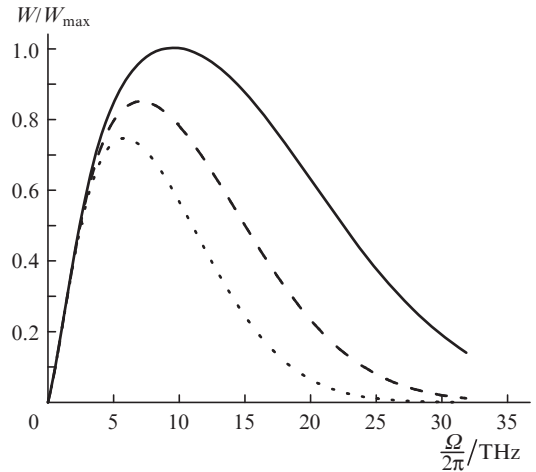


Figure 1. Spectral energy densities of low-frequency radiation upon irradiation of the gold target by a pulse with a duration of (solid line) 15, (dashed curve) 20 and (dotted curve) 25 fs.

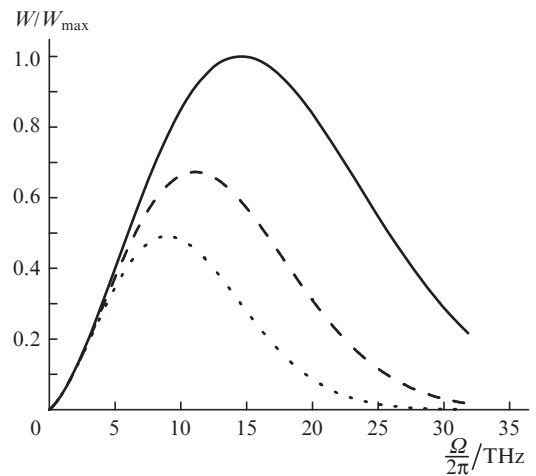


Figure 2. Spectral energy densities of low-frequency radiation upon irradiation of the aluminium target by a pulse with a duration of (solid line) 15, (dashed curve) 20 and (dotted curve) 25 fs.

maximum in the radiation spectrum takes place at a frequency of ~ 0.5 THz, which is much less than the expected value of $\sim 1/(2\pi\tau_p) \sim 5$ THz. This difference is probably due to the limited resolution of the ZnTe detector at frequencies, which are close and somewhat larger than 2.5 THz [1].

Expression (37) allows us to find the time dependence of the field at the observation point of generated radiation:

$$\begin{aligned} B_r(\mathbf{r}, t) &= \frac{1}{2\pi} \int_{-\infty}^{\infty} d\Omega \exp(-i\Omega t) B_r(\mathbf{r}, \Omega) \\ &= \frac{1}{\pi} \int_0^{\infty} d\Omega \operatorname{Re}[\exp(-i\Omega t) B_r(\mathbf{r}, \Omega)]. \end{aligned} \quad (50)$$

Because the field at the point of observation differs from the field on the metal surface only by the delay time r/c , then by integrating expression (37) over Ω , we assume $x = z = 0$. In a vacuum, $|\mathbf{E}_r| = |\mathbf{B}_r|$; therefore, after integration over Ω , in (50) we find the experimentally studied [1] dependence of the field amplitude on time. The results of numerical calculations using formulas (37) and (50) are shown in Fig. 3 for the above-mentioned parameters of the gold target and the parameters of the laser pulse used in [1]: $\lambda = 810$ nm, $t_p \simeq 50$ fs and $I_L t_p \simeq 5.8$ mJ cm $^{-2}$. The solid curve in Fig. 3 is obtained by integrating expression (37) over the entire range of frequencies. The shape of this curve is similar to the shape of the curve found in the experiment [1] and shown in Fig. 3 from paper [1]. However, according to this figure the field of the generated pulse exists during the time ~ 2 ps, which is almost an order of magnitude greater than that calculated theoretically (see Fig. 3 in this paper). This difference in the widths of the generated pulse can be eliminated, if we integrate over Ω in (50) to the frequency $\Omega \sim 2.5$ THz, which limits the frequency range well recorded by the ZnTe detector. In integrating in (50) to $\Omega < 2.5$ THz, we obtain the pulse, the width of which is comparable with that obtained in [1]. The field represented by the solid curve in Fig. 3 is produced by two sources – the current flowing along the normal to the surface and the current flowing along the surface. The contributions of each of these currents into the field are shown in Fig. 3 by dashed and

dotted curves. One can see that under the experimental conditions discussed in [1], the contributions of the currents that are proportional to J_x and J_z are comparable in magnitude. In this case, the current-induced (proportional to J_z) nonlinear polarisability {see formula (2) in [3]} used in [1] for the interpretation of data on the action of an s-polarised pulse on the gold surface leads to a time-symmetric shape of the generated low-frequency pulse (dashed curve in Fig. 3). The experimentally observed asymmetric shape of the pulse appears due to the nonlinear current along the surface taken into account (solid and dashed curves in Fig. 3), which, within the above theory, differs from zero only when account is taken of electron collisions. Equation (2) in [1] does not take into account the impact of J_x on the generated field.

Consider the energy of low-frequency radiation. From (45), (46) and (49) we obtain that at $v_s\tau_p \ll 1$, the total energy density is

$$W = \frac{8}{9} \sqrt{2\pi} \frac{I_L^2}{nmc^3} \frac{1 + v^2\tau_p^2}{\omega_p^2\tau_p} \sin^2\theta \cos^2\theta, \quad (51)$$

and at $v_s\tau_p \gg 1$, –

$$W = 4 \frac{I_L^2}{nmc^3} \frac{v^2}{\omega_p^2 v_s} \sin^2\theta \cos^2\theta. \quad (52)$$

Relations (51) and (52) allow us to assess the total energy of the low-frequency pulse. For example, for the laser pulse with an energy density $I_L \sim 10^{12}$ W cm $^{-2}$ and duration 50 fs, irradiating the gold target, from (52) we have $W \simeq 1.5 \times 10^{-14}$ J cm $^{-2}$, which corresponds to the radiation flux density $W/t_p \sim 0.3$ W cm $^{-2}$. According to relations (51) and (52), the total energy of low-frequency radiation is proportional to the square of the flux density of radiation at the fundamental frequency. At the same time, W can be estimated by using a relatively small value of I_L . The fact is that the above theory takes into account the effect of a high-frequency field on the motion of electrons in the framework of perturbation theory. This approach is certainly justified if the characteristic velocity of the electrons in the high-frequency field is less than their thermal velocity, which leads to limitation of I_L . In particular, under conditions of a high-frequency skin effect, for which we present the estimates, the energy flux density limitation has the form $I_L < 0.125cnk_B T$, where k_B is the Boltzmann constant [12]. For the gold target, when $n \simeq 6 \times 10^{22}$ cm $^{-3}$ and the electron temperature typical for the fluxes under consideration is $T > 1000$ K, we obtain $I_L < 3 \times 10^{12}$ W cm $^{-2}$.

6. Conclusions

We have presented above a relatively simple theory of generation of low-frequency radiation appearing due to the slow temporal change in the nonlinear currents generated in the metal by a femtosecond s-polarised laser pulse. We have shown that the account for the electron collisions can describe the contribution to the radiation, caused by the nonlinear current along the surface of the conducting target. This contribution determines to a large extent the shape of the generated low-frequency pulse. At higher frequencies of collisions, the nonlinear current along the surface provides a more efficient generation of low frequency radiation than the nonlinear current along the normal to the surface; as a result, there appears a significant increase in the total energy of the low-frequency pulse. The theory presented can qualitatively explain the time

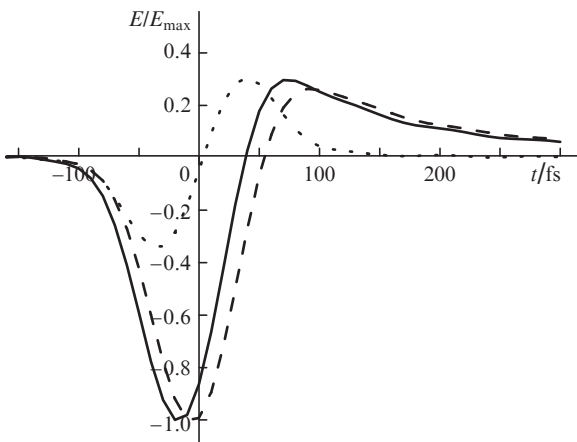


Figure 3. Field of a low-frequency pulse appearing upon irradiation of the gold target by a pulse with a duration of 50 fs (solid curve), and the fields appearing by taking into account only the nonlinear current along the surface (dashed curve) and only the current along the normal to the surface (dotted curve). The fields are normalised to the maximum of the modulus of the field, $E_{\max} = \max|E_r(\mathbf{r}, t)|$.

and frequency characteristics of terahertz radiation, obtained experimentally in [1, 2]. At the same time, obvious is the need for the further development of the theory taking into account the spatial dispersion of the metal in order to present a more adequate description of the generation of radiation at low frequencies. However, this is the subject of a separate study.

Acknowledgements. The work was supported by the RAS Presidium Programme (No. 24), Educational and Scientific Complex of FIAN and the Russian Foundation for Basic Research (Grant No. 12-02-31683-mol-a).

References

1. Kadlec F., Kužel P., Coutaz J.-L. *Opt. Lett.*, **29**, 2674 (2004).
2. Kadlec F., Kužel P., Coutaz J.-L. *Opt. Lett.*, **30**, 1402 (2005).
3. Suvorov E.V., Akhmedzhanov R.A., Fadeev D.A., Ilyakov I.E., Mironov V.A., Shishkin B.V. *Opt. Lett.*, **37**, 2520 (2012).
4. Weiss C., Wallenstein R., Beigang R. *Appl. Phys. Lett.*, **77**, 4160 (2000).
5. Welsh G.H., Wynne K. *Opt. Express*, **17**, 2470 (2009).
6. Bezhanov S.G., Uryupin S.A. *Kvantovaya Elektron.*, **40**, 495 (2010) [*Quantum Electron.*, **40**, 495 (2010)].
7. Gurzhi R.N. *Zh. Eksp. Teor. Fiz.*, **35**, 965 (1958) [*Sov. Phys. JETP*, **8**, 673 (1959)].
8. Johnson P.B., Christy R.W. *Phys. Rev. B*, **6**, 4370 (1972).
9. Kikoin I.K. (Ed.) *Tablitsy fizicheskikh velichin. Spravochnik* (Tables of Physical Quantities. Handbook) (Moscow: Atomizdat, 1976).
10. Smith D.Y., Segal B. *Phys. Rev. B*, **34**, 5191 (1986).
11. Rakić A.D. *Appl. Opt.*, **34**, 4755 (1995).
12. Isakov V.A., Kanavin A.P., Uryupin S.A. *Kvantovaya Elektron.*, **36**, 928 (2006) [*Quantum Electron.*, **36**, 928 (2006)].